

Reconstruction of the Dark Energy equation of state

J. Alberto Vázquez^{a,b} M. Bridges^{a,b} M.P. Hobson^b A.N. Lasenby^{a,b}

^aKavli Institute for Cosmology, Madingley Road, Cambridge CB3 0HA, UK.

^bAstrophysics Group, Cavendish Laboratory, JJ Thomson Avenue, Cambridge CB3 0HE, UK.

E-mail: jv292@cam.ac.uk, mb435@mrao.cam.ac.uk, mph@mrao.cam.ac.uk,
a.n.lasenby@mrao.cam.ac.uk

Abstract. One of the main challenges of modern cosmology is to investigate the nature of dark energy in our Universe. The properties of such a component are normally summarised as a perfect fluid with a (potentially) time-dependent equation-of-state parameter $w(z)$. We investigate the evolution of this parameter with redshift by performing a Bayesian analysis of current cosmological observations. We model the temporal evolution as piecewise linear in redshift between ‘nodes’, whose w -values and redshifts are allowed to vary. The optimal number of nodes is chosen by the Bayesian evidence. In this way, we can both determine the complexity supported by current data and locate any features present in $w(z)$. We compare this node-based reconstruction with some previously well-studied parameterisations: the Chevallier-Polarski-Linder (CPL), the Jassal-Bagla-Padmanabhan (JBP) and the Felice-Nesseris-Tsujikawa (FNT). By comparing the Bayesian evidence for all of these models we find an indication towards possible time-dependence in the dark energy equation-of-state. It is also worth noting that the CPL and JBP models are strongly disfavoured, whilst the FNT is just significantly disfavoured, when compared to a simple cosmological constant $w = -1$. We find that our node-based reconstruction model is slightly disfavoured with respect to the Λ CDM model.

Keywords: Equation of State, Dark Energy, Cosmological Parameters from CMBR, Bayesian Analysis

Contents

1	Introduction	1
2	Analysis	2
2.1	Nodal Reconstruction I	3
2.2	Nodal reconstruction II	5
2.3	CPL and JBP parameterisations	7
2.4	FNT parameterisation	9
3	Discussion and Conclusions	10

1 Introduction

Over the past decade, one of the most pressing goals of modern cosmology has been to explain the accelerated expansion of the Universe [1, 2]. Considerable observational and theoretical effort has been focused on understanding this remarkable phenomenon. It is often postulated that an exotic new source of stress-energy with negative pressure may be responsible for the cosmic acceleration: such a component is called *dark energy* (DE).

The dynamical properties of dark energy are normally summarised as a perfect fluid with (in general) a time-dependent equation-of-state parameter $w(z)$, defined as the ratio of its pressure to its energy density. The simplest proposal, namely a cosmological constant Λ , is described by the redshift independent $w = -1$. Alternative cosmological models that deviate from standard Λ CDM, but still lead to an accelerating Universe, include: K-essence, quintessence and non-minimally coupled scalar fields [3–6], braneworld models [7], modified gravity [8–12], interacting dark energy [13–15], anisotropic universes [16–18], amongst many others [19–26]. In the absence of a fundamental and well-defined theory of dark energy, $w(z)$ has been parameterised in a number of different ways, including: the CPL, JBP and FNT models [27–30], the Hannestad and Wetterich parameterisations [31, 32], polynomial, logarithmic and oscillatory expansions [33–35], Kink models [36], and quite a few others [37]. The *a priori* assumption of a specific model or the use of particular parameterisations can, however, lead to misleading results regarding the properties of the dark energy. Hence, some studies instead perform a direct, model-independent (‘free-form’) reconstruction of $w(z)$ from observational data, using, for instance, a principal component analysis [38–43], maximum entropy techniques [44], binning $w(z)$ in redshift space [45, 46], non-parametric approaches [47–52] and several other techniques [53–67].

In this paper we explore the possible dynamical behaviour of the dark energy based on the most minimal *a priori* assumptions. Given current cosmological observations and using the Bayesian evidence as an implementation of Occam’s razor, we select the preferred shape of $w(z)$. Our method considers possible deviations from the cosmological constant by modelling $w(z)$ as a linear interpolation between a set of ‘nodes’ with varying w -values and redshifts (in the most general case). An advantage of this method is that the number of nodes is directly chosen by the model Bayesian evidence. This reconstruction process is essentially identical to the approach used previously to recover the preferred shape of the primordial spectrum of curvature perturbations $P(k)$ [68]. For comparison, we also consider

some existing models that propose a parameterised functional form for $w(z)$, namely the CPL, JBP and FNT models. For each model we compute its evidence and, according to the Jeffreys guidelines, we select the best model preferred by the data.

The paper is organised as follows: in the next Section we describe the data sets and cosmological parameters used in the analysis. We then describe the form of existing parameterisations used by other authors and define the reconstruction used in this paper. The resulting parameter constraints and evidences for each model are then discussed. Finally, in Section 3, based on Jeffrey’s guidelines, we decide which model provides the best description for current observational data and present our conclusions.

2 Analysis

The data-sets considered throughout our analysis include temperature and polarisation measurements from the 7-year data release of the Wilkinson Microwave Anisotropy Probe (WMAP; [69]), together with the 148 GHz measurements from the Atacama Cosmology Telescope (ACT; [70]). In addition to CMB data, we include distance measurements of 557 Supernovae Ia from the Supernova Cosmology Project Union 2 compilation (SCP; [71]). We also incorporate Baryon Acoustic Oscillation (BAO; [72]) measurements of distance, and baryon density information from Big Bang Nucleosynthesis (BBN; [73]), and impose a Gaussian prior using measurements of the Hubble parameter today H_0 , from the Hubble Space Telescope key project (HST; [74]).

We consider purely Gaussian adiabatic scalar perturbations and neglect tensor contributions. We assume a flat Λ CDM universe¹ described by the following parameters: $\Omega_b h^2$ and $\Omega_{\text{DM}} h^2$ are the physical baryon and dark matter densities, respectively, relative to the critical density (h is the dimensionless Hubble parameter such that $H_0 = 100h \text{ kms}^{-1}\text{Mpc}^{-1}$), θ is $100\times$ the ratio of the sound horizon to angular diameter distance at last scattering surface, τ is the optical depth at reionisation, A_s and n_s are the amplitude of the primordial spectrum and the spectral index respectively, measured at the pivot scale $k_0 = 0.002 \text{ Mpc}^{-1}$. Aside from the Sunyaev-Zel’dovich (SZ) amplitude A_{SZ} used by WMAP analyses, the 148 GHz ACT likelihood incorporates two additional secondary parameters: the total Poisson power A_p at $l = 3000$ and the amplitude of the clustered power A_c . To describe the overall shape of the dark energy equation-of-state parameter $w(z)$ in our nodal reconstruction, we introduce a set of amplitudes w_{z_i} at determined positions z_i . The CPL and JBP models each depend upon just two parameters: w_0 and w_a ; whereas the FNT parameterisation depends upon four parameters: w_0 , w_a , τ and a_t . The assumed flat priors on the parameters of each $w(z)$ reconstruction are discussed below.

To carry out the exploration of the parameter space, we input $w(z)$ into a modified version of the CAMB code [79], which implements a parameterised post-Friedmann (PPF) prescription for the dark energy perturbations [80]. Then, we incorporate into the COSMOMC package [81] a substantially improved and fully-parallelized version of the *nested sampling* algorithm MULTINEST [82, 83]. The MULTINEST algorithm increases the sampling efficiency for calculating the evidence and allows one to obtain posterior samples even from distributions with multiple modes and/or pronounced degeneracies between parameters. The Bayes factor

¹The possibility of a dynamical dark energy in a curved universe has also been considered by, i.e. [75–78].

\mathcal{B}_{ij} , or equivalently the difference in log evidences $\ln \mathcal{Z}_i - \ln \mathcal{Z}_j$, provides a measure of how well model i fits the data compared to model j [84–87]. A suitable guideline for making qualitative conclusions has been laid out by Jeffreys [88]: if $\mathcal{B}_{ij} < 1$ model i should not be favoured over model j , $1 < \mathcal{B}_{ij} < 2.5$ constitutes significant evidence, $2.5 < \mathcal{B}_{ij} < 5$ is strong evidence, while $\mathcal{B}_{ij} > 5$ would be considered decisive.

2.1 Nodal Reconstruction I

We first perform the reconstruction of $w(z)$ by parameterising it as piecewise linear between a set of nodes with variable amplitudes (w_{z_i} -values), but with fixed, equally-spaced redshifts. Throughout, we bear in mind that current relevant information, mainly coming from SN Ia, is encompassed between the present epoch $z_{\min} = 0$ and $z_{\max} = 2$. At higher redshifts there is no substantial information to place strong constraints on dark energy, thus beyond $z > 2$ we assume $w(z)$ to be constant, with a value equal to that at z_{\max} . At each node, we allow variations in amplitudes w_{z_i} with a conservative prior $w_{z_i} = [-2, 0]$. Our description of $w(z)$ can be summarised as:

$$w(z) = \begin{cases} w_{z_{\min}} & z = 0 \\ w_{z_i} & z \in \{z_i\} \\ w_{z_{\max}} & z \geq 2 \end{cases} \quad (2.1)$$

and with linear interpolation for $0 \leq z_i < z < z_{i+1} \leq 2$.

While the use of linear interpolation between nodes may seem crude, we have shown in a previous work [68] that the use of smoothed interpolation functions, such as cubic splines, can lead to significant spurious features in the reconstruction, thus leading to poor fits to observational data and also unrepresentative errors.

We perform all of our model comparisons with respect to the simplest explanation of dark energy, namely a cosmological constant, which is specified by a redshift-independent $w = -1$. First, we consider deviations of the Λ CDM model by letting the equation-of-state parameter vary only in amplitude: $w(z) = w_0 = \text{constant}$ (see Figure 1(a)). The incorporation of two or more parameters, as in models (b) and (c) respectively, allows us to test the dark energy time-evolution. Figure 1 also includes the 1D marginalised posterior distribution for the corresponding amplitude at each node and for each reconstruction. In the top label of each model we have included the Bayes factor compared to the Λ CDM model.

In model (b), we notice the overall shape of $w(z)$ includes a slight positive tilt and a narrow waist located at $z \sim 0.3$. It is also observed that at the present epoch $w(z=0) \lesssim -1$ is slightly favoured, while at higher redshifts $w(z) \gtrsim -1$ is preferred, hence, the reconstructed $w(z)$ exhibit a crossing of the line $w = -1$. The crossing of the phantom divide line $w = -1$ (PDL), plays a key role in identifying the correct dark energy model [89]. If future surveys confirm its existence, single scalar field theories (with minimal assumptions) might be in serious problems as they cannot reproduce this essential feature, and therefore alternative models should be considered, e.g. scalar-tensor theories [90, 91], braneworld models [92, 93], $f(R)$ gravity [10–12, 94]. To continue with our reconstruction process, we then place a third point (c) midway between the two existing nodes in (b). This model mimics a running behaviour by allowing slight variations in the interpolated slopes between the three nodes. The freedom in its shape, together with the very weak constraints at high redshifts, lead to a $w(z)$ with slight negative slope at early times, in contrast to model (b). Furthermore the

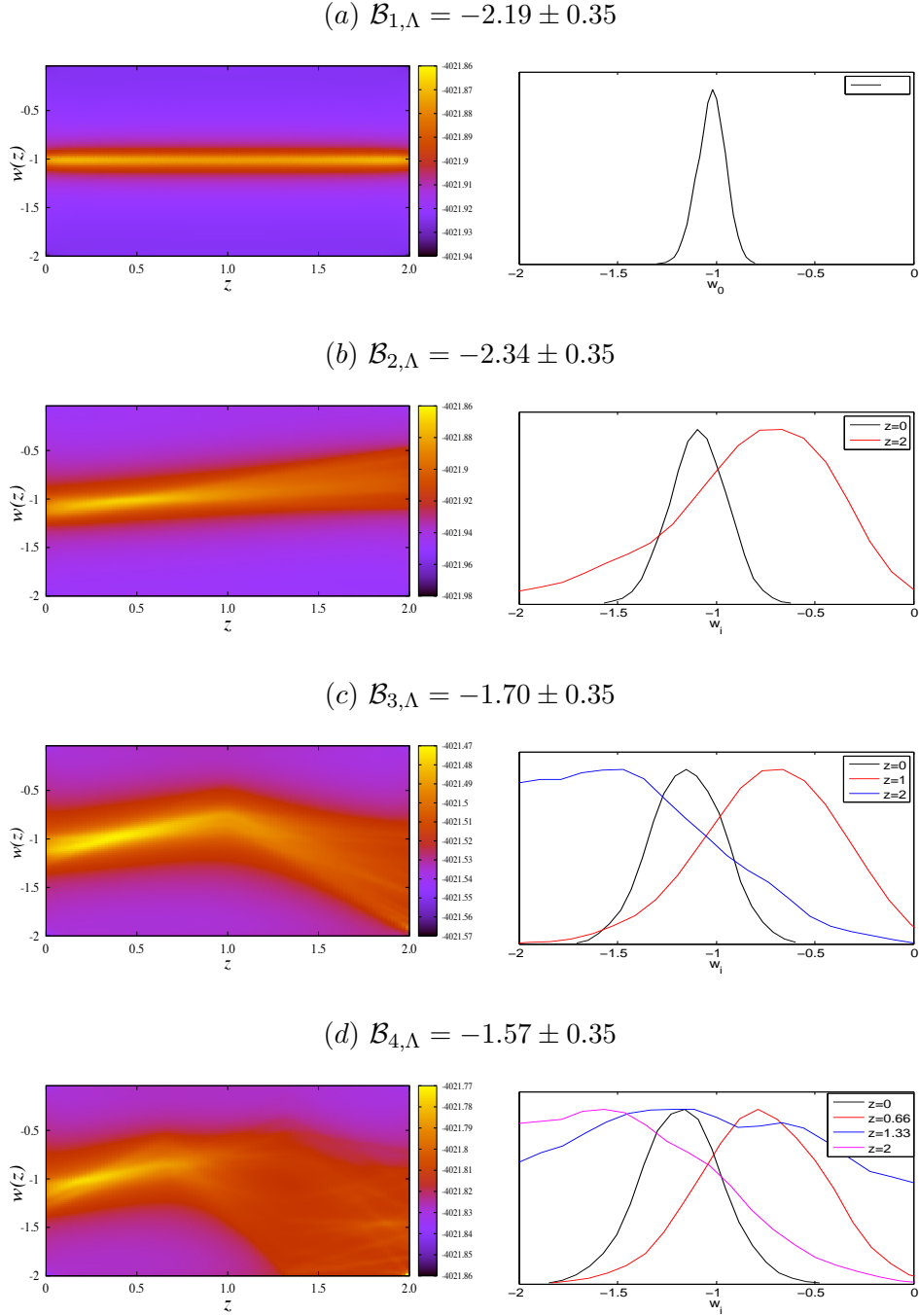


Figure 1. Left: Reconstruction of the dark energy equation-of-state parameter modelled as piecewise linear between nodes that may vary in amplitude w_i but are fixed in redshift z , showing the mean amplitude values and their corresponding 1σ error bands. The colour-code shows $\ln(\text{likelihood})$, where lighter regions represents an improved fit. Right: 1D marginalised posterior distribution of the amplitudes w_i at each z -node (shown in the right-top corner), in each reconstruction. The top label in each panel denotes the associated Bayes factor respect to the Λ CDM model.

presence of a small bump in the resulting $w(z)$ at $z \sim 1$ (see Figure 1 (c)) might point to some weak departure from the cosmological constant $w = -1$.

We can continue this process of adding more nodes but always using the Bayesian evidence to penalise any unnecessary inclusion of model parameters. The inclusion of a fourth stage with z -space split into three equally spaced regions is given by model (d). At low redshifts the shape of the equation of state is well constrained with tight error bands on each node, whereas at high redshifts the error bands again indicate the lack of sufficient data to provide strong constraints. Notice also the increased error bands due to the addition of further nodes and (anti-)correlations created between them: for instance, the posterior distribution of the amplitude w_{z_i} at $z = 0$ is broadened as the number of nodes is increased. At this stage, the evidence has flattened off, and so it seems reasonable to stop adding parameters in the reconstruction process at this point. The constraints on the w_{z_i} amplitudes used on each reconstruction are given by (for two-tailed distributions 68% C.L. are shown, whilst for one-tailed distributions the upper 95% C.L.):

- (a) $w_0 = -1.02 \pm 0.07$,
- (b) $w_{z=0} = -1.09 \pm 0.14$, $w_{z>2} = -0.83 \pm 0.39$,
- (c) $w_{z=0} = -1.14 \pm 0.17$, $w_{z=1} = -0.73 \pm 0.33$, $w_{z>2} < -0.65$,
- (d) $w_{z=0} = -1.18 \pm 0.20$, $w_{z=0.66} = -0.78 \pm 0.30$, $w_{z=1.33} = 1.03 \pm 0.53$, $w_{z>2} < -0.62$.

The models used in the reconstruction of $w(z)$ are assessed according to the Jeffreys guideline. The Bayes factor between the Λ CDM model and the one-node model $\mathcal{B}_{1,\Lambda} = -2.19 \pm 0.35$ points out that $w(z) = w_0$ (where w_0 is a free constant), is strongly disfavoured when compared to the cosmological constant, similarly, when two independent nodes are used $\mathcal{B}_{2,\Lambda} = -2.34 \pm 0.35$. Thus, parameterisations that contain one or two parameters are not able to provide an adequate description of the behaviour of $w(z)$, and hence are strongly disfavoured by current observations. The addition of nodes in the third and fourth stage provides more flexibility in the shape of the reconstructed $w(z)$. Thus, the evidence for these models shows an improvement, compared to the first and second models, indicating the possible presence of some features in the time evolution of the equation-of-state parameter. Nonetheless, when they are compared to Λ CDM, they are still marginally disfavoured: $\mathcal{B}_{3,\Lambda} = -1.70 \pm 0.35$ and $\mathcal{B}_{4,\Lambda} = -1.57 \pm 0.35$.

2.2 Nodal reconstruction II

We previously reconstructed $w(z)$ by placing nodes at particular fixed positions in z -space. However, to localise features, we now extend the analysis by also allowing the z -position of each node to move freely. In particular, we again fix two z -nodes at sufficiently separated positions $z_{\min} = 0$ and $z_{\max} = 2$, but now place inside additional ‘nodes’ with the freedom to move around in both position z_i and amplitude w_{z_i} . This method has the advantage that we do not have to specify the number and location of nodes describing $w(z)$; indeed, the form of any deviation from flat $w(z)$ can be mimicked through a change in the amplitudes and/or positions of the internal nodes. Also, the reduced number of internal nodes avoids the creation of wiggles due to high (anti-)correlation between nodes, which might lead to a misleading shape for $w(z)$. We use the same priors for the amplitudes $w_{z_i} = [-2, 0]$ as we adopted in Section 2.1. Hence, for this type of nodal-reconstruction the equation of state is

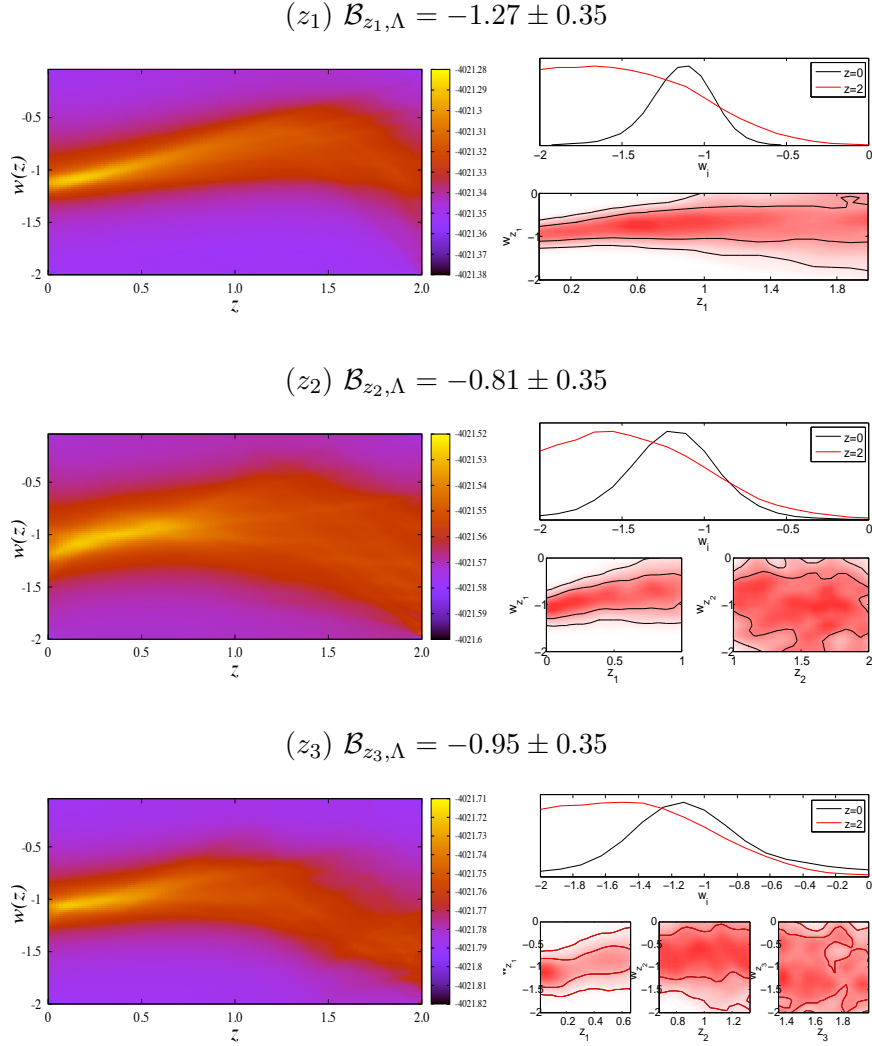


Figure 2. Left: Reconstruction of the dark energy equation-of-state parameter $w(z)$ using one-internal-node (top) and two-internal z -nodes (bottom) that move freely in both amplitude w_i and redshift z_i . Right: corresponds to the 1D and 2D marginalised posterior distribution of the amplitudes and z -node positions in each reconstruction. The colour-code indicates the $\ln(\text{Likelihood})$, where lighter regions represents an improved fit, and the top label in each panel denotes the associated Bayes factor with respect to the ΛCDM model.

described by

$$w(z) = \begin{cases} w_{z_{\min}} & z = 0 \\ w_{z_1} & 0 < z_i < z_{i+1} < 2 \\ w_{z_{\max}} & z \geq 2 \end{cases} \quad (2.2)$$

and with linear interpolation for $0 \leq z_1 < z_{i+1} \leq 2$.

Figure 2 illustrates the reconstruction of $w(z)$ from the mean posterior estimates for each node, with 1σ error bands on the amplitudes (left). Also plotted are the 1D and 2D

marginalised posterior distributions on the parameters used to describe $w(z)$ (right). The reconstructed shape for the two-internal-node model (middle panel) resembles the form obtained in Figure 1(c), but now with a turn-over shifted to earlier times. A similar turn-over has been found using principal component analysis by [40, 41]. The narrow waist at $z \sim 0.3$ is also noticeable, where the SNe constraints seem to be tightest. For the one and three-internal-nodes case (top and bottom panel of Figure 2), we observe $w(z)$ has essentially the same behaviour as in the two-internal-node model, being the preferred model. Finally, a common feature throughout all the reconstructed equation of state $w(z)$ is observed: the presence of the crossing PDL within the range $0 < z < 0.5$. The constraints on the w_{z_i} amplitudes used on each reconstruction are given by (for two-tailed distributions 68% C.L. are shown, whilst for one-tailed distributions the upper 95% C.L.):

$$\begin{aligned}
(z_1) \quad & w_{z=0} = -1.14 \pm 0.18, \quad w_{0 < z < 2} > -1.39 \pm 0.35, \quad w_{z > 2} < -0.70, \\
(z_2) \quad & w_{z=0} = -1.18 \pm 0.26, \quad w_{0 < z < 1} = -0.83 \pm 0.29, \quad w_{1 < z < 2} = 1.02 \pm 0.52, \quad w_{z > 2} < -0.63, \\
(z_3) \quad & w_{z=0} = -1.07 \pm 0.36, \quad w_{0 < z < 0.66} = -0.98 \pm 0.29, \quad w_{0.66 < z < 1.33} = -0.84 \pm 0.47, \\
& w_{1.33 < z < 2} = -1.02 \pm 0.55, \quad w_{z > 2} < 0.63.
\end{aligned}$$

The similar shape of the three models are in good agreement with their Bayes factor: $\mathcal{B}_{z_2, z_1} = +0.46 \pm 0.35$, $\mathcal{B}_{z_3, z_2} = -0.14 \pm 0.35$. According to the Jeffreys guideline, even though the two internal-node model contains more parameters, it is significantly preferred over the models with one and two fixed-nodes, i.e. $\mathcal{B}_{z_2, 2} = +1.53 \pm 0.35$. However, when compared to the cosmological constant model the Bayes factor is too small to draw any decisive conclusions: $\mathcal{B}_{z_2, \Lambda} = -0.81 \pm 0.35$. Thus we conclude that the internal-node models might be considered as viable models to characterise the dark energy dynamics. As seen in Figure 2, the Bayesian evidence has reached a plateau and thus we cease the addition of further nodes.

2.3 CPL and JBP parameterisations

In this section we examine some existing parameterised models for $w(z)$ and compare these to our nodal reconstructions. In particular, we consider the simple parameterised description introduced by Chevallier-Polarski-Linder (CPL; [27, 28]), that has the functional form:

$$w(z) = w_0 + w_a \frac{z}{1+z}, \quad (2.3)$$

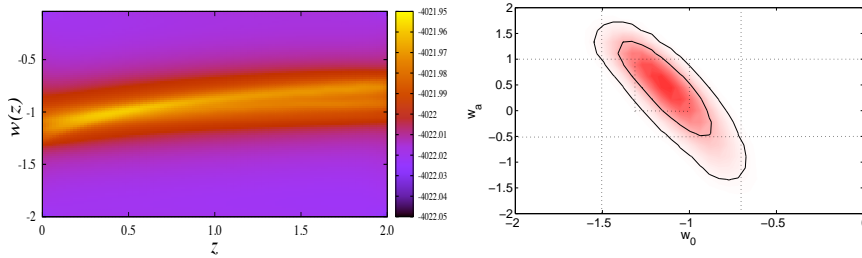
where the parameters w_0 and w_a are real numbers such that at the present epoch $w|_{z=0} = w_0$ and $dw/dz|_{z=0} = -w_a$, and as we go back in time $w(z \gg 1) \sim w_0 + w_a$. Thus, we limit the CPL parameters by the flat priors $w_0 = [-2, 0]$ and $w_a = [-3, 2]$.

We also consider the parameterisation suggested by Jassal-Bagla-Padmanabhan (JBP; [29]):

$$w(z) = w_0 + w_a \frac{z}{(1+z)^2}. \quad (2.4)$$

In this model, the parameter w_0 determines the properties of $w(z)$ at both low and high redshifts: $w(z=0) = w_0$ and $w(z \gg 1) \sim w_0$. To explore the parameter space we consider the following flat priors on the JBP parameters: $w_0 = [-2, 0]$ and $w_a = [-6, 6]$.

$$\text{(CPL)} \mathcal{B}_{\text{CPL},\Lambda} = -2.84 \pm 0.35$$



$$\text{(JBP)} \mathcal{B}_{\text{JBP},\Lambda} = -2.82 \pm 0.35$$

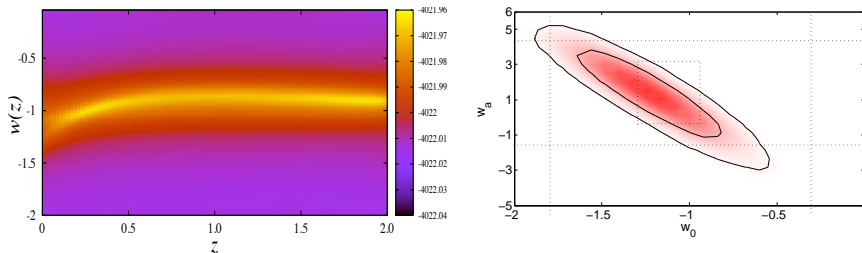


Figure 3. Reconstruction of the dark energy equation of state $w(z)$ assuming the Chevallier-Polarski-Linder (top) and the Jassal-Bagla-Padmanabhan parameterisation (bottom), along with their corresponding 2D constraints with 1σ and 2σ confidence contours (right panel). The colour-code indicates the $\ln(\text{Likelihood})$, where lighter regions represents an improved fit; the top label in each panel denotes the associated Bayes factor with respect to the ΛCDM model. Dotted lines indicate the priors choice.

Figure 3 shows 2D joint constraints, with 1σ and 2σ confidence contours, for the parameters used to describe the CPL and JBP models, and the resulting shape of $w(z)$ corresponding to the mean posterior estimates of w_0 and w_a . In each panel we have included the Bayes factor compared to the ΛCDM model. Both of the models are in good agreement with a simple cosmological constant. The current constraints for the CPL and JBP parameters are essentially as we expected:

$$\text{(CPL)} \quad w_0 = -1.11 \pm 0.17, \quad w_a = 0.34 \pm 0.60,$$

$$\text{(JBP)} \quad w_0 = -1.21 \pm 0.26, \quad w_a = 1.28 \pm 1.62.$$

Given that the CPL and JBP parameterisations depend upon just two parameters, they seem to not possess enough freedom to capture local features of $w(z)$, i.e. the CPL model does not exhibit a turn-over, see Figure 3. This is reflected in the large difference in the Bayesian evidence for this model compared to that of the cosmological constant: $\mathcal{B}_{\text{CPL},\Lambda} = -2.84 \pm 0.35$ and $\mathcal{B}_{\text{JBP},\Lambda} = -2.82 \pm 0.35$. In fact, the CPL equation of state looks similar to that obtained in Figure 1 (b), confirming our results. An important point to emphasise is that, for the chosen priors, $\mathcal{B}_{\text{CPL},z_2} = -2.03 \pm 0.35$ and $\mathcal{B}_{\text{JBP},z_2} = -2.01 \pm 0.35$, indicating that both models are strongly disfavoured in comparison to the internal-node re-

Table 1. Robustness of the CPL and JBP models over small variations of the prior range. The associated Bayes factor in each model is compared with respect to the Λ CDM model.

Prior	$\mathcal{B}_{\text{CPL},\Lambda}$	Prior	$\mathcal{B}_{\text{JBP},\Lambda}$
w_0, w_a		w_0, w_a	
$[-1.5, -0.7], [-3, 2]$	-1.84 ± 0.35	$[-1.8, -0.6], [-6, 6]$	-2.35 ± 0.35
$[2, 0], [-0.5, 1]$	-2.11 ± 0.35	$[-2, 0], [-1, 4]$	-1.82 ± 0.35
$[-1.5, -0.7], [-0.5, 1]$	-1.39 ± 0.35	$[-1.8, -0.6], [-1, 4]$	-1.51 ± 0.35
$[-1.3, -1], [0, 1]$	-0.26 ± 0.35	$[-1.4, -1.1], [0, 3]$	-0.54 ± 0.35

construction, shown in Figure 2.

To illustrate the robustness of the model to small variations of the prior range, we compute the Bayesian evidence using different sets of priors, shown in Table 1; the prior ranges are illustrated with dotted lines in Figure 3. The reader will observe that even though the priors, in the first three choices, have been shrunk to within the region of the 2σ contours, the Bayes factor still disfavors significantly both the CPL and JBP parameterisations compared to the cosmological constant and the two-internal-node reconstruction. With respect to the extremely small prior (last row of Table 1), we notice that the JBP model does not contain the cosmological constant $w_0 = -1$. Its Bayes factor compared to the Λ CDM model $\mathcal{B}_{\text{JBP},\Lambda} = -0.54 \pm 0.35$, shows that models with $w(z=0) \lesssim -1.1$ might provide a good description for the current state of the Universe.

2.4 FNT parameterisation

We have observed that two-parameter functions are not, in general, sufficient to recover the evolution of the dark energy $w(z)$, obtained previously in the reconstruction process. As an alternative to the CPL and JBP functional form, we consider a more general parameterisation introduced by Felice-Nesseris-Tsujikawa (FNT, [30]), which allows fast transitions for the dark energy equation of state:

$$w(a) = w_a + (w_0 - w_a) \frac{a^{1/\tau} [1 - (a/a_t)^{1/\tau}]}{1 - a_t^{-1/\tau}}, \quad (2.5)$$

where $a = 1/(1+z)$, $a_t > 0$ and $\tau > 0$. The parameter w_0 determines the $w(a)$ properties at present time $w_0 = w(a=1)$, whereas w_a the asymptotic past $w_a = w(a \ll 1)$. In this model, the equation of state $w(a)$ has an extremum at $a_* = a_t/2^\tau$ with value

$$w(a_*) = w_p + \frac{1}{4} \frac{(w_0 - w_a) a_t^{1/\tau}}{1 - a_t^{-1/\tau}}. \quad (2.6)$$

Based on the assumptions given by [30], we explore the cosmological parameter-space using the following flat priors: $w_0 = [-2, 0]$, $w_a = [-2, 0]$, $a_t = [0, 1]$ and $\tau = [0, 1]$, using a full Monte-Carlo exploration. We leave the analysis of the robustness of this model under small variations on the priors, for a future work.

$$\text{(FNT)} \quad \mathcal{B}_{\text{FNT},\Lambda} = -1.68 \pm 0.35$$

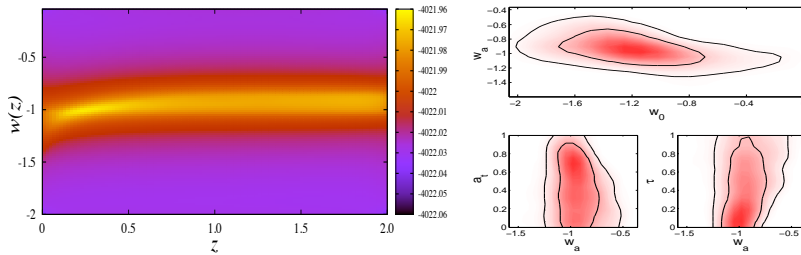


Figure 4. Reconstruction of the dark energy equation of state $w(z)$ assuming the Felice-Nesseris-Tsujikawa paramterisation (left panel), along with their corresponding 1D, and 2D constraints with 1σ and 2σ confidence contours (right panel). The colour-code indicates the $\ln(\text{Likelihood})$, where lighter regions represents an improved fit; the top label in the panel denotes the associated Bayes factor with respect to the ΛCDM model.

In Figure 4 we plot 2D joint constraints, with 1σ and 2σ confidence contours, for the parameters used to describe the FNT model, and its corresponding reconstruction of $w(z)$. We observe that the FNT model is in good agreement with a simple cosmological constant $w(z) = -1$, with current constraints:

$$\text{(FNT)} \quad w_0 = -1.19 \pm 0.32, \quad w_a = -0.94 \pm 0.15.$$

Given that the best-fit values of w_0 and w_a are very similar, the second term on the left hand side of (2.6) is almost negligible. This results in essentially unconstrained values for a_t and τ , and so w_a becomes the dominant term in the dynamics of $w(z)$. We have found that the FNT model shares a similar feature common throughout all the models: $w(z=0) \lesssim w(z \gg 1)$, in agreement with our previous results. The best-fit form of $w(z)$ presents a maximum value given by $w(a_*) = -0.95$ located at $z_* = 1/a_* - 1 = 1.59$. On the other hand, the top label of Figure 4 shows the Bayes factor compared to the ΛCDM model: $\mathcal{B}_{\text{FNT},\Lambda} = -1.68 \pm 0.35$. That is, the FNT model improves on the Evidence computed from the CPL and JBP models, however the inclusion of twice the number of parameters makes it significantly disfavored when compared to the cosmological constant $w(z) = -1$, and indistinguishable compared to our node-base reconstruction, i.e. $\mathcal{B}_{\text{FNT},z_2} = -0.82 \pm 0.35$.

3 Discussion and Conclusions

The major task for present and future dark energy surveys is to determine whether dark energy is evolving in time. Using the latest cosmological datasets (SN, CMB and LSS), we have performed a Bayesian analysis to extract the general form of the dark energy equation-of-state parameter, employing an optimal nodal reconstruction where $w(z)$ is interpolated linearly between a set of nodes with varying w_{z_i} -values and redshifts. Our method has the advantage that the number and location of nodes are directly chosen by the Bayesian evidence. We have also explored standard parameterisations which include the CPL, JBP and FNT models. We find our results to be generally consistent with the cosmological constant scenario, however

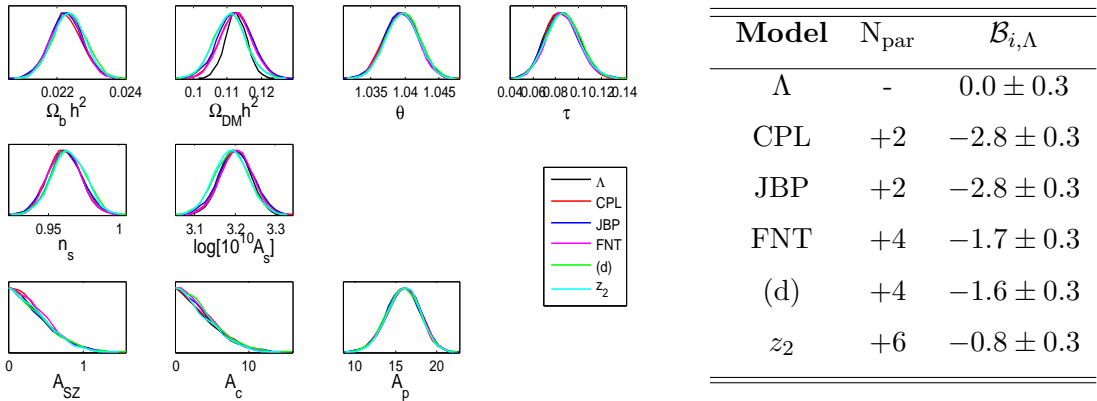


Figure 5. Left: 1D marginalised posterior distributions of the standard cosmological parameters, of each corresponding model listed in the right table. Right: comparison of the Bayes factor $\mathcal{B}_{i,\Lambda}$ for some selected models with an extra-number of parameters N_{par} . Each description is compared respect to the Λ CDM model.

the dark energy does seem to exhibit a temporal evolution, although very weak. Besides the cosmological constant, the preferred $w(z)$ has $w \lesssim -1$ at the present time and a small bump located at $z \sim 1.3$, whereas at redshifts $z \gtrsim 1.5$ the accuracy of current data is not enough to place effective constraints on different parameterisations. It is also interesting to note the presence of a narrow waist in many models, situated at $z \sim 0.3$, which is where the constraints on $w(z)$ are tightest. A dominant feature throughout the reconstruction is the presence of the crossing of the PDL $w = -1$, obtained within the range $0 < z < 0.5$. Within the GR context, this phantom crossing cannot be produced by single (quintessence or phantom) scalar fields. Hence, if future surveys confirm its evidence, multiple fields or additional interactions should be taken into account to reproduce this important behaviour.

All the models considered share a consistent set of primary cosmological parameters: $\Omega_b h^2$, $\Omega_{\text{DM}} h^2$, θ , τ , n_s , A_s , in addition to secondary parameters: A_{SZ} , A_p , A_c . The marginalised posterior distributions for these parameters are consistent with those obtained using only the concordance Λ CDM model. In Figure 5, we plot 1D posterior distributions of the cosmological parameters for some selected models. We observe that their values remain well constrained despite the freedom in $w(z)$. The only noticeable change is in the dark matter parameter, where the Λ CDM model displays the tightest constraints. In the same figure we include the corresponding Bayes factors, all of which are quoted relative to the cosmological constant model. The preferred Bayesian description of the $w(z)$ is provided by the Λ CDM model, followed by the two-internal-node model z_2 , introduced in this work. It is important to note that the CPL and JBP models, each with two parameters, are not able to provide an adequate description for the behaviour of $w(z)$, and are hence strongly disfavoured using the priors chosen. The FNT model with four parameters, from which two of them remained unconstrained, is significantly disfavoured. We stress that for the smallest prior range, the Bayes factor for the JBP model (which does not include the case $w_0 = -1$) is indistinguishable from that of the Λ CDM model, therefore pointing to a possible departure from the cosmological constant.

Acknowledgments

This work was carried out largely on the Cambridge High Performance Computing cluster, DARWIN. JAV is supported by CONACYT México.

References

- [1] S. Perlmutter and *et. al.* Measurements of Omega and Lambda from 42 High-Redshift Supernovae. *The Astrophysical Journal*, 517(2):565, 1999.
- [2] A. G. Riess and *et. al.* Observational Evidence from Suernovae for an Accelerating Universe and a Cosmological Constant. *The Astronomical Journal*, 116(3):1009, 1998.
- [3] B. Ratra and P. J. E. Peebles. Cosmological consequences of a rolling homogeneous scalar field. *Phys. Rev. D*, 37:3406–3427, Jun 1988.
- [4] C. Armendariz-Picon, V. Mukhanov, and P. J. Steinhardt. Dynamical Solution to the Problem of a Small Cosmological Constant and Late-Time Cosmic Acceleration. *Phys. Rev. Lett.*, 85:4438–4441, Nov 2000.
- [5] A. Vikman. Can dark energy evolve to the phantom? *Phys. Rev. D*, 71:023515, Jan 2005.
- [6] L.A. Urena and T. Matos. New Cosmological Tracker Solution for Quintessence *Phys. Rev. D*, 62:061301(R), 2000.
- [7] R. Maartens. Brane-world gravity. *Living Reviews in Relativity*, 7(7), 2004.
- [8] S. Capozziello. Curvature quintessence. *Int.J.Mod.Phys.*, D11:483–492, 2002.
- [9] S. Nojiri and S. D. Odintsov. Modified $f(R)$ gravity consistent with realistic cosmology: From a matter dominated epoch to a dark energy universe. *Phys. Rev. D*, 74:086005, Oct 2006.
- [10] S. A. Appleby and R. A. Battye. Do consistent models mimic general relativity plus Λ ? *Physics Letters B*, 654(1–2):7 – 12, 2007.
- [11] W. Hu and I. Sawicki. Models of $f(r)$ cosmic acceleration that evade solar system tests. *Phys. Rev. D*, 76:064004, Sep 2007.
- [12] A. Starobinsky. Disappearing cosmological constant in $f(R)$ gravity. *JETP Letters*, 86:157–163, 2007. 10.1134/S0021364007150027.
- [13] L. Amendola, G. C. Campos, and R. Rosenfeld. Consequences of dark matter-dark energy interaction on cosmological parameters derived from type Ia supernova data. *Phys. Rev. D*, 75:083506, Apr 2007.
- [14] T. Clemson, K. Koyama, G.-B. Zhao, R. Maartens, and J. Väliviita. Interacting dark energy: Constraints and degeneracies. *Phys. Rev. D*, 85:043007, Feb 2012.
- [15] J. Lu, Y. Wu, Y. Jin, and Y. Wang. Investigate the interaction between dark matter and dark energy. [arXiv:1203.4905], 03 2012.
- [16] Ö. Akarsu and C. Klnç. Bianchi type III models with anisotropic dark energy. *General Relativity and Gravitation*, 42:763–775, 2010. 10.1007/s10714-009-0878-7.
- [17] V. Marra, M. Paakkonen, and W. Valkenburg. Bias on w from large-scale structure. [arXiv:1203.2180], 2012.
- [18] W. Valkenburg. Perceiving the equation of state of Dark Energy while living in a Cold Spot. *Journal of Cosmology and Astroparticle Physics*, 2012(01):047, 2012.
- [19] R. R. Caldwell, R. Dave, and P. J. Steinhardt. Cosmological Imprint of an Energy Component with General Equation of State. *Phys. Rev. Lett.*, 80:1582–1585, Feb 1998.

- [20] V. Sahni and S. Habib. Does Inflationary Particle Production Suggest $\Omega_m > 1$. *Phys. Rev. Lett.*, 81:1766–1769, Aug 1998.
- [21] I. Zlatev, L. Wang, and P. J. Steinhardt. Quintessence, Cosmic Coincidence, and the Cosmological Constant. *Phys. Rev. Lett.*, 82:896–899, Feb 1999.
- [22] S. Matarrese, C. Baccigalupi, and F. Perrotta. Approaching λ without fine-tuning. *Phys. Rev. D*, 70:061301, Sep 2004.
- [23] V. Pettorino, C. Baccigalupi, and F. Perrotta. Scaling solutions in scalar–tensor cosmologies. *Journal of Cosmology and Astroparticle Physics*, 2005(12):003, 2005.
- [24] G. Gupta, E. N. Saridakis, and A. A. Sen. Nonminimal quintessence and phantom with nearly flat potentials. *Phys. Rev. D*, 79:123013, Jun 2009.
- [25] J. L. Cervantes-Cota, R. de Putter, and E. V. Linder. Induced gravity and the attractor dynamics of dark energy/dark matter. *Journal of Cosmology and Astroparticle Physics*, 2010(12):019, 2010.
- [26] A. de la Macorra. Scalar Field Dark Energy Parametrization. [arXiv:1108.0876], 2011.
- [27] M. Chevallier and D. Polarski. Accelerating Universes with Scaling Dark Matter. *International Journal of Modern Physics D*, 10(2):213–223, 2001.
- [28] E. V. Linder. Exploring the Expansion History of the Universe. *Phys. Rev. Lett.*, 90:091301, Mar 2003.
- [29] H. K. Jassal, J. S. Bagla, and T. Padmanabhan. WMAP constraints on low redshift evolution of dark energy. *Monthly Notices of the Royal Astronomical Society: Letters*, 356(1):L11–L16, 2005.
- [30] A. de Felice, S. Nesseris, and S. Tsujikawa. Observational constraints on dark energy with a fast varying equation of state. [arXiv:1203.6760], 2012.
- [31] S. Hannestad and E. Mörtsell. Cosmological constraints on the dark energy equation of state and its evolution. *Journal of Cosmology and Astroparticle Physics*, 2004(09):001, 2004.
- [32] C. Wetterich. Phenomenological parameterization of quintessence. *Physics Letters B*, 594(1–2):17 – 22, 2004.
- [33] J.-Z. Ma and X. Zhang. Probing the dynamics of dark energy with novel parametrizations. *Physics Letters B*, 699(4):233 – 238, 2011.
- [34] I. Sendra and R. Lazkoz. SN and BAO constraints on (new) polynomial dark energy parametrizations: current results and forecasts. [arXiv:1105.4943], 05 2011.
- [35] Q.-J. Zhang and Y.-L. Wu. Modelling Time-varying Dark Energy with Constraints from Latest Observations. [arXiv:1103.1953], 2011.
- [36] B. A. Bassett, P. S. Corasaniti, and M. Kunz. The Essence of Quintessence and the Cost of Compression. *The Astrophysical Journal Letters*, 617(1):L1, 2004.
- [37] A. Shafieloo, V. Sahni and A. Starobinsky. Is cosmic acceleration slowing down? *Phys. Rev. D*, 80:101301(R), 2009.
- [38] D. Huterer and G. Starkman. Parametrization of Dark-Energy Properties: A Principal-Component Approach. *Phys. Rev. Lett.*, 90:031301, Jan 2003.
- [39] G.-B. Zhao, D. Huterer, and X. Zhang. High-resolution temporal constraints on the dynamics of dark energy. *Phys. Rev. D*, 77:121302, Jun 2008.
- [40] P. Serra, A. Cooray, D. E. Holz, A. Melchiorri, S. Pandolfi, and D. Sarkar. No evidence for dark energy dynamics from a global analysis of cosmological data. *Phys. Rev. D*, 80:121302, Dec 2009.

- [41] Y. Gong, R.-G. Cai, Y. Chen, and Z.-H. Zhu. Observational constraint on dynamical evolution of dark energy. *Journal of Cosmology and Astroparticle Physics*, 2010(01):019, 2010.
- [42] G.-B. Zhao and X. Zhang. Probing dark energy dynamics from current and future cosmological observations. *Phys. Rev. D*, 81:043518, Feb 2010.
- [43] Ishida, E. E. O. and de Souza, R. S. Hubble parameter reconstruction from a principal component analysis: minimizing the bias. *A&A*, 527:A49, 2011.
- [44] C. Zunckel and R. Trotta. Reconstructing the history of dark energy using maximum entropy. *Monthly Notices of the Royal Astronomical Society*, 380(3):865–876, 2007.
- [45] R. de Putter and E. V. Linder. To bin or not to bin: Decorrelating the cosmic equation of state. *Astroparticle Physics*, 29(6):424 – 441, 2008.
- [46] R. Lazkoz, V. Salzano, and I. Sendra. Revisiting a model-independent dark energy reconstruction method. [arXiv:1202.4689], 02 2012.
- [47] A. Shafieloo, U. Alam, V. Sahni, and A. A. Starobinsky. Smoothing supernova data to reconstruct the expansion history of the Universe and its age. *Monthly Notices of the Royal Astronomical Society*, 366(3):1081–1095, 2006.
- [48] T. Holsclaw, U. Alam, B. Sansó, H. Lee, K. Heitmann, S. Habib, and D. Higdon. Nonparametric reconstruction of the Dark Energy Equation of State. *Phys. Rev. D*, 82:103502, Nov 2010.
- [49] T. Holsclaw, U. Alam, B. Sansó, H. Lee, K. Heitmann, S. Habib, and D. Higdon. Nonparametric Dark Energy reconstruction from Supernova Data. *Phys. Rev. Lett.*, 105:241302, Dec 2010.
- [50] M. Seikel, C. Clarkson, and M. Smith. Reconstruction of dark energy and expansion dynamics using Gaussian processes. [arXiv:1204.2832], 2012.
- [51] A. Shafieloo. Crossing Statistic: Reconstructing the Expansion History of the Universe. [arXiv:1204.1109], 2012.
- [52] A. Shafieloo, A. G. Kim, and E. V. Linder. Gaussian process Cosmography. [arXiv:1204.2272], 2012.
- [53] T. Chiba and T. Nakamura. Feasibility of reconstructing the quintessential potential using type ia supernova data. *Phys. Rev. D*, 62:121301, Nov 2000.
- [54] T. D. Saini, S. Raychaudhury, V. Sahni, and A. A. Starobinsky. Reconstructing the Cosmic Equation of State from Supernova Distances. *Phys. Rev. Lett.*, 85:1162–1165, Aug 2000.
- [55] D. Huterer and M. S. Turner. Probing dark energy: Methods and strategies. *Phys. Rev. D*, 64:123527, Nov 2001.
- [56] J. Weller and A. Albrecht. Future supernovae observations as a probe of dark energy. *Phys. Rev. D*, 65:103512, May 2002.
- [57] R. A. Daly and S. G. Djorgovski. A model-independent determination of the expansion and acceleration rates of the Universe as a function of redshift and constraints on Dark Energy. *The Astrophysical Journal*, 597(1):9, 2003.
- [58] U. Alam, V. Sahni, T. Deep Saini, and A. A. Starobinsky. Exploring the expanding universe and dark energy using the statefinder diagnostic. *Monthly Notices of the Royal Astronomical Society*, 344(4):1057–1074, 2003.
- [59] Y. Wang and M. Tegmark. New Dark Energy constraints from Supernovae, Microwave Background, and Galaxy Clustering. *Phys. Rev. Lett.*, 92:241302, Jun 2004.
- [60] U. Alam, V. Sahni, T. Deep Saini, and A. A. Starobinsky. Is there supernova evidence for dark energy metamorphosis? *Monthly Notices of the Royal Astronomical Society*,

354(1):275–291, 2004.

- [61] D. Huterer and A. Cooray. Uncorrelated estimates of dark energy evolution. *Phys. Rev. D*, 71:023506, Jan 2005.
- [62] E. V. Linder and D. Huterer. How many dark energy parameters? *Phys. Rev. D*, 72:043509, Aug 2005.
- [63] Y. Wang and M. Tegmark. Uncorrelated measurements of the cosmic expansion history and dark energy from supernovae. *Phys. Rev. D*, 71:103513, May 2005.
- [64] V. Sahni and A. Starobinsky. Reconstructing Dark Energy. *International Journal of Modern Physics D*, 15(12):2105–2132, 2006.
- [65] U. Alam, V. Sahni, and A. A. Starobinsky. Exploring the properties of dark energy using type-ia supernovae and other datasets. *Journal of Cosmology and Astroparticle Physics*, 2007(02):011, 2007.
- [66] V. Sahni, A. Shafieloo, and A. A. Starobinsky. Two new diagnostics of dark energy. *Phys. Rev. D*, 78:103502, Nov 2008.
- [67] D. Rubin and *et. al.* Looking Beyond Lambda with the Union Supernova Compilation. *The Astrophysical Journal*, 695(1):391, 2009.
- [68] J. A. Vazquez, M. Bridges, M. Hobson, and A. Lasenby. Model selection applied to reconstruction of the Primordial Power Spectrum. *Journal of Cosmology and Astroparticle Physics*, 2012(06):06, 2012.
- [69] E. Komatsu and *et. al.* Seven-year Wilkinson Microwave Anisotropy Probe (WMAP) Observations: Cosmological Interpretation. *The Astrophysical Journal Supplement Series*, 192(2):18, 2011.
- [70] J. Dunkley and *et. al.* The Atacama Cosmology Telescope: Cosmological Parameters from the 2008 Power Spectra. [arXiv:1009.0866], 2010.
- [71] R. Amanullah and *et. al.* Spectra and Hubble Space Telescope Light Curves of Six Type Ia Supernovae at $0.511 < z < 1.12$ and the Union2 Compilation. *The Astrophysical Journal*, 716(1):712, 2010.
- [72] W. J. Percival and *et. al.* Baryon acoustic oscillations in the Sloan Digital Sky Survey Data Release 7 galaxy sample. *Monthly Notices of the Royal Astronomical Society*, 401(4):2148–2168, 2010.
- [73] S. Burles, K. M. Nollett, and M. S. Turner. Big Bang Nucleosynthesis Predictions for Precision Cosmology. *The Astrophysical Journal Letters*, 552(1):L1, 2001.
- [74] A. G. Riess and *et. al.* A Redetermination of the Hubble Constant with the Hubble Space Telescope from a Differential Distance Ladder. *The Astrophysical Journal*, 699(1):539, 2009.
- [75] R. Hlozek, M. Cortés, C. Clarkson, and B. Bassett. Dark energy degeneracies in the background dynamics. *General Relativity and Gravitation*, 40:285–300, 2008.
- [76] Y. Gong, X.-m. Zhu, and Z.-H. Zhu. Current cosmological constraints on the curvature, dark energy and modified gravity. *Monthly Notices of the Royal Astronomical Society*, 415(2):1943–1949, 2011.
- [77] N. Pan, Y. Gong, Y. Chen, and Z.-H. Zhu. Improved cosmological constraints on the curvature and equation of state of dark energy. *Classical and Quantum Gravity*, 27(15):155015, 2010.
- [78] Y. Wang and P. Mukherjee. Observational constraints on dark energy and cosmic curvature. *Phys. Rev. D*, 76:103533, Nov 2007.
- [79] A. Lewis, A. Challinor, and A. Lasenby. Efficient Computation of Cosmic Microwave

Background Anisotropies in Closed Friedmann-Robertson-Walker Models. *The Astrophysical Journal*, 538(2):473, 2000.

- [80] W. Fang, W. Hu, and A. Lewis. Crossing the phantom divide with parametrized post-Friedmann dark energy. *Phys. Rev. D*, 78:087303, Oct 2008.
- [81] A. Lewis and S. Bridle. Cosmological parameters from CMB and other data: A Monte Carlo approach. *Physical Review D*, 66(10), 2002.
- [82] F. Feroz and M. P. Hobson. Multimodal nested sampling: an efficient and robust alternative to Markov Chain Monte Carlo methods for astronomical data analyses. *Monthly Notices of the Royal Astronomical Society*, 384(2):449–463, 2008.
- [83] F. Feroz, M. P. Hobson, and M. Bridges. MultiNest: an efficient and robust Bayesian inference tool for cosmology and particle physics. *Monthly Notices of the Royal Astronomical Society*, 398(4):1601–1614, 2009.
- [84] T. D. Saini, J. Weller, and S. L. Bridle. Revealing the nature of dark energy using Bayesian evidence. *Monthly Notices of the Royal Astronomical Society*, 348(2):603–608, 2004.
- [85] C. Gordon and R. Trotta. Bayesian calibrated significance levels applied to the spectral tilt and hemispherical asymmetry. *Monthly Notices of the Royal Astronomical Society*, 382(4):1859–1863, 2007.
- [86] R. Trotta. Bayes in the sky: Bayesian inference and model selection in cosmology. *Contemporary Physics*, 49(2):71–104, 2008.
- [87] J. A. Vazquez, A. N. Lasenby, M. Bridges and M.P. Hobson. A Bayesian study of the primordial power spectrum from a novel closed universe model *Monthly Notices of the Royal Astronomical Society*, 442:1948–1956, 2012.
- [88] H. Jeffreys. *Theory of Probability*. Oxford University Press, 1998.
- [89] H. Zhang. Crossing the phantom divide. [arXiv:0909.3013], 2009.
- [90] B. Boisseau, G. Esposito-Farèse, D. Polarski, and A. A. Starobinsky. Reconstruction of a Scalar-Tensor Theory of gravity in an Accelerating Universe. *Phys. Rev. Lett.*, 85:2236–2239, Sep 2000.
- [91] C. Deffayet, O. Pujolàs, I. Sawicki, and A. Vikman. Imperfect dark energy from kinetic gravity braiding. *Journal of Cosmology and Astroparticle Physics*, 2010(10):026, 2010.
- [92] L. P. Chimento, R. Lazkoz, R. Maartens, and I. Quiros. Crossing the phantom divide without phantom matter. *Journal of Cosmology and Astroparticle Physics*, 2006(09):004, 2006.
- [93] V. Sahni and Y. Shtanov. Braneworld models of dark energy. *Journal of Cosmology and Astroparticle Physics*, 2003(11):014, 2003.
- [94] H. Motohashi, A. A. Starobinsky, and J. Yokoyama. f(R) Gravity and its Cosmological Implications. *Int.J.Mod.Phys.*, D20:1347–1355, 2011.